Eur. Phys. J. B **36**, 15–20 (2003)
DOI: 10.1140/epjb/e2003-00312-3

THE EUROPEAN PHYSICAL JOURNAL B

Predicted spin-orbit coupling effect on the magnetic ordering of crystalline uranium dioxide

J.C. Boettger[a]

Applied Physics Division, Los Alamos National Laboratory, Los Alamos, NM 87545, USA

Received 3 March 2003 / Received in final form 9 August 2003
Published online 19 November 2003 –

Abstract. The magnetic ordering of fluorite structure uranium dioxide has been investigated using fully-relativistic linear combinations of Gaussian type orbitals - fitting function (LCGTO-FF) calculations, within the generalized gradient approximation (GGA) to density functional theory. Three types of collinear spin-orderings were considered; ferromagnetic with spins aligned in the (001) direction and two antiferromagnetic (001) layer structures with spins aligned either perpendicular to each plane (001) or parallel to each plane (100). For each ordering, the total energy and spin-moment were calculated both with and without spin-orbit coupling. The ferromagnetic ordering is found to be energetically preferred to the antiferromagnetic orderings, contrary to experiment, whether or not spin-orbit coupling is included. Spin-orbit coupling is shown to have a significant quenching effect on the spin-moment and also introduces a strong magnetic anisotropy in the antiferromagnetic state that favors the (001) alignment over the (100) alignment.

PACS. 71.15.Rf Relativistic effects – 75.25.+z Spin arrangements in magnetically ordered materials (including neutron and spin-polarized electron studies, synchrotron-source X-ray scattering, etc.) – 75.50.Ee Antiferromagnetics – 75.30.Gw Magnetic anisotropy – 64.30.+t Equations of state of specific substances

1 Background

Fluorite structure uranium dioxide (UO_2) is of long-standing interest to materials scientists due to its technological value as a nuclear reactor fuel and heterogeneous catalyst. UO_2 also is known to be a highly-reactive toxic contaminant, which may appear in the environment either in its crystalline form or as an oxide-layer formed on metallic uranium. As a result, the electronic structure of bulk UO_2 has been the subject of much experimental research over the last two decades. Those measurements reveal that the energy bands of UO_2, near the Fermi level, may be divided into three distinct regions: (1) A valence band of mixed O($2p$), U($5f$), and U($6d$) character, ranging from 8 to 4 eV below the Fermi level, which provides most of the bonding [1,2]; (2) A nearly dispersionless band containing two well-localized U($5f$) electrons, that lies roughly 1.5 eV below the Fermi level [1,2]; and (3) A conduction band that begins 1 eV above the Fermi level [3] with mostly U($5f$) character, changing to U($6d$) character at higher energies [4]. The dispersionless U($5f$) band and the bottom of the conduction band represent the bottom and top of a 2.5 eV band gap; i.e., UO_2 is insulating. Detailed analysis of core photoemission spectra [5] suggests that UO_2 is a prototypical Mott-Hubbard-type insulator, with a $5f$ to $5f$ band gap [6,7]. In addition, it is well-established that UO_2 becomes a noncollinear antiferromagnet below 30.8 K [8–10].

The complicated combination of physical effects manifested by UO_2 (highly-correlated electron effects, noncollinear antiferromagnetism, and large relativistic effects) poses a severe challenge for electronic structure theorists. In fact, although a number of density functional theory [11,12] (DFT) electronic structure calculations have been carried out on UO_2, [4,13–20] none has realistically accounted for all of the observed effects. Those calculations may be divided into two categories: (1) "Traditional" DFT calculations using either the local density approximation [21] (LDA) or the generalized gradient approximation [22] (GGA), neither of which adequately describes the highly-correlated nature of the $5f$ electrons; and (2) LDA+U calculations [23] which approximate the highly-correlated electron effects by adding a strong Coulomb repulsion term, U, to a standard LDA calculation, but have not yet included density gradient corrections or spin-orbit coupling (SOC) effects in the particular case of UO_2.

One common failing of all calculations, to date, is that none of them has simultaneously included both spin-polarization and SOC effects, although both of those effects are known [19,20] to be important individually. This deficiency is particularly unfortunate, because the existence of noncollinear magnetism depends on the spin-anisotropy provided by SOC. In addition, even at the

[a] e-mail: jn@lanl.gov

scalar-relativistic level, the correct DFT prediction for the magnetic ordering in UO_2 has not been clearly established, with one LDA calculation [17] predicting an antiferromagnetic ground state at the ambient volume and two recent GGA calculations [19,20] predicting a ferromagnetic ground state at that volume.

To address those issues, the magnetic ordering in fluorite structure UO_2 has been investigated, within the collinear spin approximation, using the GGA model and a relativistic variant [24–27] of the linear combinations of Gaussian type orbitals - fitting function (LCGTO-FF) technique [28,29], as embodied in the program package GTOFF [30]. Three types of magnetic order were considered; ferromagnetic with the spins aligned in the (001) direction and two distinct antiferromagnetic (001) layer structures with spins aligned either perpendicular to each plane, in the (001) direction, or parallel to each plane, in the (100) direction. For each ordering, the total energy and spin-moment were calculated both with and without SOC included, clearly revealing the impact of SOC on the spin-polarization in UO_2.

In the next section, the relativistic LCGTO-FF method will be described, including the implementation of simultaneous collinear spin-polarization and SOC. Next, a few computational details will be discussed. The results obtained here for the magnetic orderings and the zero-pressure properties of UO_2 will be presented in the fourth section. Concluding remarks will be given in the final section.

2 Theoretical background

The LCGTO-FF method [28,29], as implemented in the crystalline electronic structure code GTOFF [30], is distinguished from other variants of the LCGTO methodology through its use of two independent auxiliary GTO basis sets to expand the charge density and exchange-correlation (XC) integral kernels; here using the GGA model. The charge fit coefficients are determined variationally, by minimizing the error in the Coulomb energy, while the XC coefficients are obtained from a least squares fit. The program GTOFF references the XC fit to the fitted density, thereby achieving a substantial speedup of the calculations, relative to other implementations of the LCGTO-FF method that use the exact density in the XC fit. In its nonrelativistic form, this implementation of the LCGTO-FF method has been in use for nearly two decades and is known to produce results that agree well with results from other all-electron, full-potential DFT electronic structure methods.

During the last five years, the LCGTO-FF method implemented in GTOFF has been extended [24–27] to include relativistic effects at progressively more realistic levels of approximation. Scalar-relativity was initially incorporated [24] using an incomplete, nuclear-only Douglas-Kroll-Hess (nDKH) transformation [31,32], that neglected all terms involving cross-products of the momentum operator [33]. That implementation was subsequently extended to include all of the scalar-relativistic cross-product terms and SOC terms produced by the nDKH transformation [25], allowing the first fully-relativistic LCGTO-FF calculations for the light-actinide metals [26]. Although the nDKH transformation has been demonstrated to produce reliable scalar-relativistic results for both atoms and solids that compare favorably with other state-of-the-art electronic structure methods, it also was shown to consistently overestimate SOC effects [27]. That specific limitation was overcome through the development of the screened-nuclear-spin-orbit (SNSO) approximation [27], which approximately includes two-electron SOC effects, without increasing the computational requirements, relative to the nDKH approximation.

The one-electron equation associated with the fully-relativistic nDKH+SNSO approximation described above, and implemented in GTOFF, may be written as

$$\left[h_{\rm KS} + \Delta h_{\rm nDKH} + \Delta h_{\rm SNSO}\right]\phi_i = \epsilon_i \phi_i. \tag{1}$$

In equation (1), the first term on the lhs is the standard nonrelativistic Kohn-Sham operator [12]

$$h_{\rm KS} = \frac{p^2}{2m} + v_{\mathit{eff}} \tag{2}$$

where

$$v_{\mathit{eff}} = v_n + v_e + v_{xc} \tag{3}$$

is the effective one-electron potential formed from the nuclear potential v_n, the electronic Coulomb potential v_e, and the DFT exchange-correlation (XC) potential v_{xc}. The second operator on the lhs of Equation (1) is the relativistic correction operator obtained from the nDKH approximation [31,32],

$$\begin{aligned}\Delta h_{\rm nDKH} = &\left[E_p - \frac{p^2}{2m}\right] + A_p\left[v_n + R_p v_n R_p\right]A_p \\ &- \frac{1}{2}(E_p W^2 + W^2 E_p + 2W E_p W) - v_n\end{aligned}$$

where

$$E_p = c(p^2 + m^2c^2)^{\frac{1}{2}}, \tag{4}$$

$$A_p = \left[\frac{E_p + mc^2}{2E_p}\right]^{\frac{1}{2}}, \tag{5}$$

$$R_p = K_p\,\sigma\cdot\mathbf{p}, \tag{6}$$

$$K_p = c/(E_p + mc^2), \tag{7}$$

and W can be expressed in momentum-space as

$$W_{p,p'} = A_p(R_p - R_{p'})A_{p'}\left[\frac{v_n(\mathbf{p},\mathbf{p}')}{E_p + E_{p'}}\right], \tag{8}$$

with $v_n(\mathbf{p},\mathbf{p}')$ being the momentum-space representation of v_n. The final operator on the lhs of equation 1 is the two-electron SOC operator obtained from the SNSO approximation [27],

$$\Delta h_{\rm SNSO}(i,j) = -\sqrt{\frac{Q(l_i)}{Z_i}}\,h_{\rm nSO}\sqrt{\frac{Q(l_j)}{Z_j}} \tag{9}$$

where i and j are basis function indices, Z_i is the nuclear charge associated with the center of basis function i, $h_{\rm nSO}$ is the nuclear-only SOC term embedded in $\Delta h_{\rm nDKH}$, and $Q(l_i)$ is a basis function dependent operator given by;

$$Q(l_i = 0, 1, 2, 3, \cdots) = 0, 2, 10, 28, \cdots \qquad (10)$$

The nDKH+SNSO approximation, expressed in equation (1), has been shown to produce reliable results for large Z materials that are more stable numerically than results obtained using more conventional DFT electronic structure methods [27]. In addition, it has been demonstrated [27] that the SNSO approximation produces spin-orbit splittings of atomic levels that are in better agreement with the splittings obtained from a numerical solution of the four-component Dirac-Kohn-Sham equation.

To date, no periodic LCGTO-FF calculation has simultaneously included both spin-polarization and SOC effects. This is not due to any fundamental limitation of the methodology, however. In fact, there has been at least one example of a fully-relativistic LCGTO-FF calculation on isolated atoms and diatomic molecules [34], that included noncollinear spin-polarization. For this investigation, GTOFF has been extended to allow simultaneous spin-polarization and SOC effects within the collinear spin approximation, in which a spin polarization axis is specified a priori and the off-diagonal spin-density $\rho_{\alpha,\beta}$, relative to the chosen axis, is then assumed to be zero. This rather limited extension to the LCGTO-FF method is straightforward to implement, since it is analogous to the treatment of spin-polarization in the nonrelativistic case [28], with the one exception that each orbital becomes a mixture of the two spin-states α and β. An extension of GTOFF to include noncollinear spin-polarization would require fitting the off-diagonal spin-density $\rho_{\alpha,\beta}$ in addition to the diagonal densities $\rho_{\alpha,\alpha}$ and $\rho_{\beta,\beta}$. In the present context, such an extension would not be particularly useful, because the primitive unit cell for the experimentally observed noncollinear antiferromagnetic ground state contains too many atoms to be computationally tractable with GTOFF, at this time.

3 Computational details

All of the magnetic orderings considered here have been modelled using a single (001) layered structure containing two formula units per primitive cell, thereby ensuring consistency between the various calculations. For the nonmagnetic and ferromagnetic systems, the two uranium atoms (and the four oxygen atoms) in each primitive cell are forced to be equivalent. For the antiferromagnetic structures, the spins of the two uranium atoms in the unit cell are assumed to have opposite spins, that are aligned either in the (001) direction, perpendicular to the atomic layers, or in the (100) direction, parallel to the atomic layers. The antiferromagnetic (100) spin structure modelled here is identical to the structure used in the earlier LDA calculation [17] on UO_2 that predicted an antiferromagnetic ground state. Note that, in the absence of SOC, the energies and spin-moments are independent of the polarization axis, as has been confirmed here with test calculations.

To ensure high quality results, relatively rich GTO basis sets, developed during previous work [19,20], were used here. The orbital basis set used for uranium began with a $23s20p15d11f$ GTO basis set that was derived from the atomic basis set of Minami and Matsuoka [35]. That primitive basis set was then reduced to a $17s14p11d7f$ basis set by contracting the more local GTOs of each l-type with coefficients obtained from a scalar-relativistic GGA atom calculation. This use of a so-called "scalar relativistic basis" is standard practice in most fully-relativistic DFT crystal calculations today. The specific orbital basis set size and the contraction pattern used here for uranium were carefully tested for a plutonium atom in reference [27] to ensure that the calculated atomic SOC splittings were well-converged and agreed well with results from a numerical solution to the full four-component Dirac-Kohn-Sham equation. The orbital basis set for oxygen was a $12s7p1d$ GTO basis set, derived from the $11s7p$ atomic basis set of van Duijneveldt [36], contracted into a $7s4p1d$ basis, using coefficients from a scalar-relativistic GGA atom calculation. The charge/XC basis sets used for uranium and oxygen were $25s/21s$ and $9s/9s$, respectively. All of these basis sets can be obtained from the author. For the magnetically ordered systems, the charge fitting functions associated with the various atoms in each unit cell were contracted, so as to impose the desired spin-ordering.

In all calculations, a uniform $4 \times 4 \times 2$ Brillouin zone (BZ) mesh was used. That mesh was reduced to 12 or 14 irreducible k-points for the antiferromagnetic systems with their spins aligned in the (001) or (100) directions, respectively. For simplicity, the nonmagnetic and ferromagnetic calculations used the same 12 point mesh as the antiferromagnetic (001) calculations. All required BZ integrations were carried out here using a Gaussian broadened histogram technique with a broadening parameter of 2 mRy. Comparison of the lattice constants and bulk moduli found here for nonmagnetic and ferromagnetic UO_2 with results from previous calculations using much denser meshes [19,20] suggests that the BZ meshes are well converged for bulk properties. (Note, however, that these meshes will not be adequate to produce accurate density of states plots.) Since the difference in energy between the two antiferromagnetic orientations is quite small, the BZ mesh was further tested by recalculating that difference at one lattice constant (10.34 au) using a $6 \times 6 \times 3$ BZ mesh. This enrichment of the mesh only altered the energy difference by 0.06 mRy, out of 0.71 mRy, again indicating good convergence. The self-consistent field (SCF) cycle for each calculation was iterated until the total energy was stable to within about 0.01 mRy.

For the ferromagnetic systems, the total spin-moment per formula unit was determined by integrating the difference between the α and β spin-densities of states, up to the Fermi level. For the antiferromagnetic systems, the spin-moment calculations become more complicated, due to the need to obtain moments for individual atoms.

From symmetry, the total spin-moment for each oxygen atom must be zero and the moments of the two uranium atoms must be equal in magnitude but opposite in direction. Even with those constraints, the division of the spin-densities between the uranium atoms is ill-defined, at best, and a number of partitioning techniques have been used in the past. In the prior LDA calculation on UO_2 [17], the spin-moment for each uranium atom was estimated by integrating the spin-densities over the atomic sphere surrounding that atom. Another related technique, often used in muffin-tin-based methods, relies on integrating the spin-densities over the muffin-tin-sphere associated with the atom of interest; yielding a lower bound to the spin-moment. In the present calculations, the antiferromagnetic spin-moment per formula unit was calculated by summing the difference between the coefficients of the s-type α and β charge fit functions centered on one of the uranium atoms. This procedure should yield an upper bound to the spin-moment. For test purposes, the spin-moment of each uranium atom was also determined by the muffin-tin-sphere method, described above, to obtain a lower bound.

4 Results

For each magnetic ordering, electronic structure calculations were carried out, both with and without SOC, for fluorite structure lattice constants ranging from 10.0 bohr to 10.5 bohr, in increments of 0.1 bohr. An additional set of calculations was carried out at the experimental lattice constant, 10.34 bohr [37]. The zero-pressure lattice constant (a), bulk modulus (B), and pressure derivative of the bulk modulus (B') were determined for each case by fitting the calculated energies with the stabilized jellium equation of state (SJEOS) of Alchagirov et al. [38]. Those zero-pressure results are listed in Table 1, along with the binding energy of the magnetic systems (E_{sp}) relative to the appropriate nonmagnetic system. The energy for each magnetic ordering is plotted as a function of lattice constant in Figures 1 (without SOC) and 2 (with SOC). The points in the figures are from the electronic structure calculations, while the lines are from the fits. The good agreement between the points and the fitted lines demonstrates the high quality of the SJEOS fits and the overall numerical stability of the LCGTO-FF method, as implemented in GTOFF.

Inspection of the spin-polarization energies listed in Table 1 reveals that the ferromagnetic structure is preferred energetically to the two antiferromagnetic structures, whether or not SOC is included, contrary to experiment [8–10]. This result does not imply any fundamental disagreement between the present results and the previous LDA calculation [17] that predicted an antiferromagnetic ground state at the experimental lattice constant, since the previous calculation did not consider ferromagnetic spin-polarization. A comparison of the spin-polarization energies for the two antiferromagnetic structures considered here also reveals a rather strong SOC-induced anisotropy, with the (001) alignment being preferred to the (100) alignment.

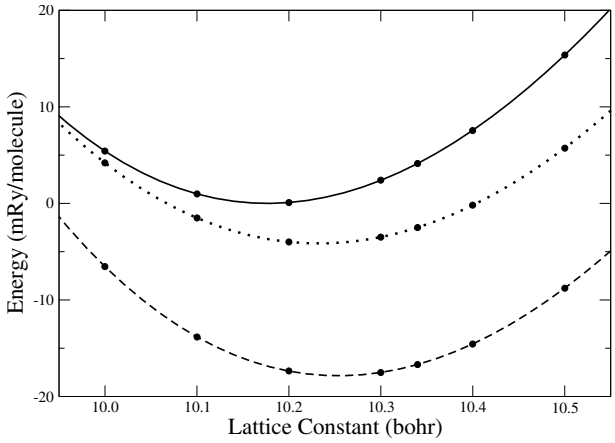

Fig. 1. Energies (mRy/molecule) versus lattice constant (bohr) for the various magnetic structures without spin-orbit coupling; solid line – nonmagnetic, dashed line – ferromagnetic, dotted line – antiferromagnetic. The energies are referenced to the fitted zero-pressure energy for nonmagnetic UO_2. Lines are from SJEOS fits.

Table 1. Theoretical lattice parameters (a; bohr), bulk moduli (B; GPa), pressure derivatives of bulk moduli (B'), spin-polarization energies (E_{sp}; mRy/molecule), and magnetic moments (μ; μ_B) are listed for UO_2, both with and without spin-orbit coupling (SOC) included; NM → nonmagnetic, FM → (001) ferromagnetism, AFM(001) → (001) antiferromagnetism, and AFM(100) → (100) antiferromagnetism. Note that the results without SOC do not depend on the polarization axis for the spins. Experimental values from reference [37] are given for a and B.

Order	SOC	a	B	B'	E_{sp}	μ
NM	no	10.18	210	4.39	0.0	0.0
FM	no	10.25	206	4.23	–17.8	2.0
AFM	no	10.23	187	3.33	–4.1	1.4
NM	yes	10.23	197	4.31	0.0	0.0
FM	yes	10.26	186	2.99	–1.9	1.5
AFM(001)	yes	10.24	186	3.31	–0.6	0.9
AFM(100)	yes	10.23	187	4.86	–0.1	0.3
Expt		10.34	213			

The lattice parameters and bulk moduli listed in Table 1 for the nonmagnetic systems, both with and without SOC, and for the ferromagnetic system, without SOC, are in excellent agreement with the results of previous LCGTO-FF GGA calculations [19,20], despite the use of a larger unit cell and coarser BZ scan in the present work. In the previous work, the lattice constant and bulk modulus that would be obtained in a calculation including both SOC and ferromagnetism were estimated by assuming that the individual effects were additive. The present results, however, clearly demonstrate that that assumption was incorrect. Instead, the effects of spin-polarization, whether ferromagnetic or antiferromagnetic, are quite small for all of the calculations that include SOC, due to a partial suppression of the spin-polarization.

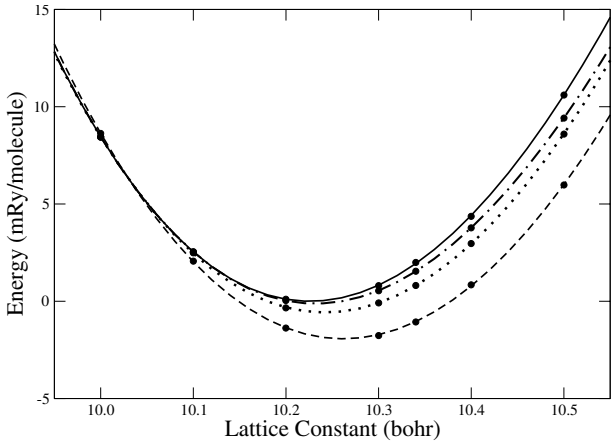

Fig. 2. Energies (mRy/molecule) versus lattice constant (bohr) for the various magnetic structures with spin-orbit coupling; solid line – nonmagnetic, dashed line – ferromagnetic (001), dotted line – antiferromagnetic (001), dash-dot line – antiferromagnetic (100). The energies are referenced to the fitted zero-pressure energy for nonmagnetic UO_2. Lines are from SJEOS fits.

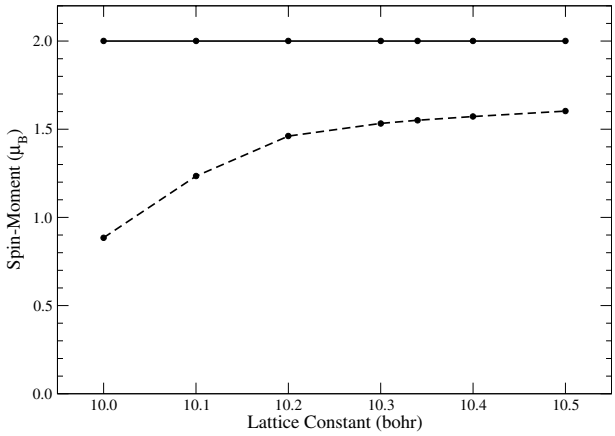

Fig. 3. Spin-moment (μ_B) versus lattice constant (bohr) for ferromagnetic UO_2, without (solid line) and with (dashed line) spin-orbit coupling (SOC). The moments are aligned in the (001) direction. Lines are guides to the eye only.

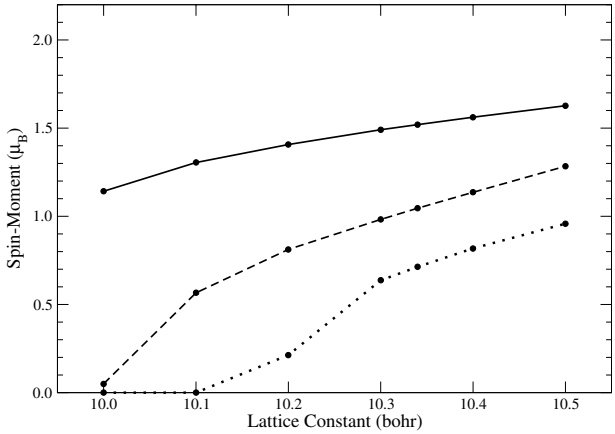

Fig. 4. Spin-moment (μ_B) versus lattice constant (bohr) for antiferromagnetic UO_2, with and without spin-orbit coupling (SOC). Without SOC (solid line) the moments do not depend on the alignment. With SOC, the moments are aligned in either the (001) direction (dashed line) or in the (100) direction (dotted line). Lines are guides to the eye only.

(Note for example the SOC-induced reduction in E_{sp} for the various magnetic systems.) This result suggests that nonmagnetic calculations, including SOC, could be used to study the zero-pressure properties of bulk UO_2, without any significant loss in accuracy relative to spin-polarized calculations.

The results in Table 1 indicate that the "best" GGA values for the lattice constant and bulk modulus of UO_2 are 10.26 bohr and 186 GPa, from the ferromagnetic calculations. Those results are in reasonable agreement with the experimental room temperature values, 10.34 bohr and 213 GPa [37], despite the failure of the GGA calculations to predict the experimentally observed magnetic order [8–10]. (Note that the agreement between the lattice constants would be even better if thermal effects were removed from the experimental value.) This result suggests that, as has been noted before [19,20], any proposed remedy for the Mott-Hubbard insulator problem in UO_2 should not increase the predicted zero-pressure lattice constant by more than a few percent. One somewhat surprising result is that the inclusion of SOC in the ferromagnetic calculations produces a deterioration in the agreement between the theoretical and experimental bulk moduli, reducing B from 206 GPa to 186 GPa. This result suggests that SOC and electron-localization effects in B tend to counteract each other. It is thus reasonable to anticipate that any future remedy to the Mott-Hubbard problem in UO_2 will increase the bulk modulus by more than 10%.

The spin-moments per formula unit (μ) calculated here, with and without SOC, are shown as functions of lattice constant in Figures 3 and 4 for the ferromagnetic and antiferromagnetic structures, respectively. The zero-pressure spin-moment for each structure was then estimated using linear interpolation; see Table 1. Comparison of the antiferromagnetic spin-moment curve obtained here without SOC (Fig. 4; solid line) with the equivalent curve in Figure 4 of reference [17] reveals a reasonable level of agreement, given the difference between the DFT models used in the calculations. In particular, the present calculations, without SOC, predict an antiferromagnetic moment of 1.52 μ_B at the measured lattice constant, while the earlier LDA calculation yielded roughly 1.49 μ_B. If the muffin-tin method had been used here to determine the spin-moment, instead of the charge fitting coefficient method, the calculated spin-moment would become 1.47 μ_B. This level of agreement between the various calculations, lends credence to the overall validity of the approximation technique being used here.

The spin-moment curves shown in Figures 3 and 4 dramatically illustrate the large effect that SOC has on the magnetic properties of UO_2, as was noted in the earlier discussion. First, SOC has a significant quenching effect on the spin-moment, regardless of the magnetic

structure, due to the SOC-induced mixing of α and β spins in each orbital. Second, SOC introduces a strong magnetic anisotropy in the antiferromagnetic state, with the (001) alignment having a larger spin-moment and spin-polarization energy than the (100) alignment. This strong anisotropy may play an important role in the formation of the true noncollinear antiferromagnetic ground state. It should be noted, however, that the well-known failure of standard DFT models to correctly predict the Mott-Hubbard insulating behavior in UO_2 is not affected by including SOC or by altering the magnetic structure; i.e., all of the present DFT calculations produce a metallic ground state in UO_2.

5 Conclusions

Simultaneous collinear spin-polarization and SOC has been successfully implemented in an all-electron LCGTO-type electronic structure program for periodic systems. That program has been used to carry out the first fully-relativistic spin-polarized electronic structure calculations on fluorite structure UO_2. Three types of collinear spin-orderings were considered; ferromagnetic with spins aligned in the (001) direction and two antiferromagnetic (001) layer structures with spins aligned either perpendicular to each plane (001) or parallel to each plane (100). The ferromagnetic order was found to be energetically preferred to the antiferromagnetic order, with or without SOC, contrary to experiment [8–10]. SOC was shown to have a significant quenching effect on the spin-moment and to introduce a strong magnetic anisotropy in the antiferromagnetic state, stabilizing the (001) polarization relative to the (100) polarization.

This work was supported by the US Department of Energy under contract W-7405-ENG-36. Partial support was provided by the LDRD program at Los Alamos National Laboratory.

References

1. A.J. Arko, D.D. Koelling, A.M. Boring, W.P. Ellis, L.E. Cox, J. Less-Common Metals **122**, 95 (1986); and references therein
2. L.E. Cox, W.P. Ellis, R.D. Cowan, J.W. Allen, S.J. Oh, I. Lindau, B.B. Pate, A.J. Arko, Phys. Rev. B **35**, 5761 (1987)
3. Y. Baer, J. Schoenes, Sol. State Comm. **33**, 885 (1980)
4. F. Jollet, T. Petit, S. Gota, N. Thromat, M. Gautier-Soyer, A. Pasturel, J. Phys. Condens. Matter **9**, 9393 (1997); and references therein
5. A. Kotani, T. Yamazaki, Prog. Theo. Phys. Suppl. **108**, 117 (1992)
6. N.F. Mott, *Metal-Insulator Transitions* (Taylor and Francis, London, 1974)
7. J. Hubbard, Proc. Roy. Soc. (London) A **276**, 238 (1963); ibid. A **281**, 401 (1964)
8. J. Faber, G.H. Lander, Phys. Rev. B **14**, 1151 (1976)
9. R. Caciuffo, G. Amoretti, P. Santini, G.H. Lander, J. Kulda, P. de V. Du Plessis, Phys. Rev. B **59**, 13892 (1999)
10. K. Ikushima, S. Tsutsui, Y. Haga, H. Yasuoka, R.E. Walstedt, N.M. Masaki, A. Nakamura, S. Nasu, Y. Onuki, Phys. Rev. B **63**, 104404 (2001)
11. P. Hohenberg, W. Kohn, Phys. Rev. B **136**, 864 (1964)
12. W. Kohn, L.J. Sham, Phys. Rev. A **140**, 1133 (1965)
13. P.J. Kelly, M.S.S. Brooks, J. Phys. C: Solid State Phys. **13**, L939 (1980)
14. M.S.S. Brooks, P.J. Kelly, Solid State Comm. **45**, 689 (1983)
15. P.J. Kelly, M.S.S. Brooks, J. Chem. Soc., Faraday Trans. **83**, 1189 (1987)
16. T. Petit, B. Morel, C. Lemaignan, A. Pasturel, B. Bigot, Phil. Mag. B **73**, 893 (1996)
17. S.L. Dudarev, D. Nguyen Manh, A.P. Sutton, Phil. Mag. B **75**, 613 (1997)
18. S.L. Dudarev, G.A. Botton, S.Y. Sasarov, Z. Szotek, W.M. Temmerman, A.P. Sutton, Phys. Stat. Solid (a) **166**, 429 (1998)
19. J.C. Boettger, A.K. Ray, Internat. J. Quantum Chem. **80**, 824 (2000)
20. J.C. Boettger, A.K. Ray, Internat. J. Quantum Chem. **90**, 1407 (2002)
21. L. Hedin, B.I. Lundqvist, J. Phys. C **4**, 2064 (1971)
22. J.P. Perdew, in *Electronic Structure of Solids*, edited by P. Ziesche, H. Eschrig (Academic Verlag, Berlin, 1991), pp. 11–20
23. V.I. Anisimov, J. Zaanen, O.K. Andersen, Phys. Rev. B **44**, 943 (1991); V.I. Anisimov, I.V. Solovyev, M.A. Korotin, M.T. Czyzyk, G.A. Sawatzky, Phys. Rev. B **48**, 16929 (1993); A.I. Liechtenstein, V.I. Anisimov, J. Zaanen, Phys. Rev. B **52**, R5467 (1995)
24. J.C. Boettger, Phys. Rev. B **57**, 8743 (1998)
25. J.C. Boettger (unpublished)
26. M.D. Jones, J.C. Boettger, R.C. Albers, D.J. Singh, Phys. Rev. B **61**, 4644 (2000)
27. J.C. Boettger, Phys. Rev. B **62**, 7809 (2000)
28. J.C. Boettger, Int. J. Quantum Chem. Symp. **27**, 147 (1993); J.C. Boettger, S.B. Trickey, Phys. Rev. B **32**, 1356 (1985); J.W. Mintmire, J.R. Sabin, S.B. Trickey, Phys. Rev. B **26**, 1743 (1982)
29. U. Birkenheuer, J.C. Boettger, N. Rösch, J. Chem. Phys. **100**, 6826 (1994); U. Birkenheuer, dissertation, TU München (1994)
30. J.C. Boettger, Int. J. Quantum Chem. Symp. **29**, 197 (1995)
31. M. Douglas, N.M. Kroll, Ann. Phys. **82**, 89 (1974)
32. B.A. Hess, Phys. Rev. A **33**, 3742 (1986); G. Jansen, B.A. Hess, Phys. Rev. A **39**, 6016 (1989); N.J.M. Geipel, B.A. Hess, Chem. Phys. Lett. **273**, 62 (1997)
33. N. Rösch, O.D. Häberlen, J. Chem. Phys. **96**, 6322 (1992); O.D. Häberlen, N. Rösch, Chem. Phys. Lett. **199**, 491 (1992); O.D. Häberlen, Ph.D. thesis, Technische Universität München, 1993
34. M. Mayer, S. Krüger, N. Rösch, J. Chem. Phys. **115**, 4411 (2001)
35. T. Minami, O. Matsuoka, Theo. Chim. Acta **90**, 27 (1995)
36. F.B. van Duijneveldt, IBM Research Report RJ945, unpublished (1971)
37. *CRC Handbook of Chemistry and Physics*, 3rd electronic edn., edited by D.R. Lide (CRC Press, Inc., Boca Raton, 2001)
38. A.B. Alchagirov, J.P. Perdew, J.C. Boettger, R.C. Albers, C. Fiolhais, Phys. Rev. B **63**, 224115 (2001)